Magna Scientia Advanced Research and Reviews

eISSN: 2582-9394

Cross Ref DOI: 10.30574/msarr

Journal homepage: https://magnascientiapub.com/journals/msarr/

(RESEARCH ARTICLE)

Check for updates

Solid lipid nanoparticles for transdermal delivery of curcumin: Optimization using factorial design and in vitro characterization

Jalal Basha [1], Y Anand Kumar [1,*] and Shamshuddin M [2]

[1] *Department of Pharmaceutics, V. L. College of Pharmacy, Raichur, Karnataka, India.*
[2] *Department of Pharmacology, V. L. College of Pharmacy, Raichur, Karnataka, India.*

Magna Scientia Advanced Research and Reviews, 2025, 13(01), 113-128

Publication history: Received on 02 December 2024; revised on 12 January 2025; accepted on 15 January 2025

Article DOI: https://doi.org/10.30574/msarr.2025.13.1.0014

Abstract

This study aimed to design and optimize Curcumin (CUR) loaded solid lipid nanoparticle (SLNs) transdermal formulations by nano emulsion template method. A 3 factor, 2 level Box-Behnken design was used to evaluate the effect of three independent variables viz., Amount of Span 60 (X1), Tween 60 (X2) and Stearyl alcohol (X3) on dependent variables viz., Particle size (Y1), entrapment efficiency (Y2) and zeta potential (Y3). Optimization study signifies that amount of formulation components viz., Span 60, Tween 60 and Stearyl alcohol influence the vesicle size, entrapment efficiency and Zeta potential. The numerical optimization was validated within the design space. The OP-CUR-SLNs exhibited good entrapment efficiency and particle size. Further the OP-CUR-SLNs loaded transdermal carbopol gel shows good *in vitro* drug release and better *ex vivo* permeation than the plain CUR loaded gel, which concludes CUR-SLNs considered to be a successful topical transdermal drug delivery system and provide a sustained release of encapsulated drug. Furthermore, CUR-SLNs loaded carbopol gel considered to be non-irritant and safe to be applied on the skin for the intended period of time.

Keywords: Curcumin; Span 60; Tween 60; BBD; ANOVA; *Ex vivo*; Skin irritation

1. Introduction

Curcumin (CUR) has wide pharmacological effects viz., antibacterial, anti-inflammatory, antioxidant, and antitumor properties[1-7]. Chemically CUR is diferuloylmethane belongs to the polyphenol class[8-10], and approved as a safe compound by World Health Organization and US Food and Drug Administration (FDA). CUR is poorly soluble belongs to BCS class IV drug, exhibiting log P value of 3.2 (absorbed approximately 60% in the gastrointestinal tract) and undergoes extensive hepatic first-pass metabolism, which leads to poor bioavailability. Therefore, it would be advantageous to enhance the aqueous solubility of CUR to develop more efficient dosage forms. Various approaches have been reported to increase the aqueous solubility by conjugating water-soluble polymers[11], liposomes[12], liquid crystals[13], nano-emulsions[14], and phospholipid complexes[15].

Solid lipid nanoparticle (SLNs) systems appear to be an efficient approach for increasing the aqueous solubility and stability of drugs and decreasing the particle size to the nanoscale level[16-19]. Further SLNs have emerged as an alternative colloidal carrier due to their advantages such as enhanced physical stability, good tolerability, ease of scale up and growth. SLNs have been widely used for the distribution of skin due to their safe interaction with skin layers and improved skin permeation[20-22].

The transdermal drug delivery system (TDDS) has attracted extensive attention due to its tremendous advantages. On one hand, it is capable to escape undesirable metabolism both in the gastrointestinal tract and in the liver after

* Corresponding author: Y Anand Kumar

traditional oral administration, not only producing a tunable drug release, but also allowing enhanced drug absorption, eventually leading to boost drug bioavailability. On the other hand, TDDS also possesses numerous benefits compared to the parenteral administrations, particularly the painless and easily operated self-administration process with higher patient compliance[23]. However, the efficacy of the transdermal drug delivery in maintaining a therapeutic level depends on the ability of the drug to penetrate the skin in adequate amounts. The barrier nature of the stratum corneum (SC) is a major challenge that restricts the entry of most drugs via the transdermal route. Many transdermal methods have been tried to achieve greater transdermal permeability in order to overcome the barrier of SC. These techniques are designed for a longer period to deliver the drug, nanotechnology has developed attractive niche research in transdermal drug delivery[24]. The present work was aimed to formulate and optimize CUR loaded SLNs comprising Span 60, Tween 60 and Stearyl alcohol through response surface Box-Behnken Design (BBD) using Design Expert® Trial Version 13. The effect of lipid mixture and surfactant composition on particle size, entrapment efficiency, *in vitro* drug release and *ex vivo* permeation behavior of CUR-SLNs loaded transdermal systems were investigated.

2. Materials and Methods

Curcumin (CUR) (Mylan Laboratories, Hyderabad), Span 60, Tween 80 (S.D Fine- Chem ltd, Mumbai). Brij 35 (Hi Media Laboratories Pvt. Ltd. Mumbai), Stearyl alcohol (Yarrow Chem products, Mumbai), Carpool (Yarrow Chem products, Mumbai) were procured. All other solvents and chemicals were used of analytical grade.

2.1. Methods

The DoE approach was applied for optimization by response surface design viz., Box-Behnken Design (BBD) using Design Expert® Trial Version 13. The BBD is an effective method of indicating the relative significance of a number of variables and their interactions. In this design 2^3 factorial design was used at 3 center points with 12 non center point experimental trials. The trials were formulated and further subjected for evaluation. BBD and the regression analysis was used to optimize the influence of independent variables viz., concentration of Span 60 (X1), Tween 60 (X2) and Stearyl alcohol (X3) on the dependent variable viz., % EE (Y1), Particle size (Y2) and Zeta potential (Y3). The design and possible formula trials were shown in tables 1, 2 and second order polynomial equation was generated as,

$$Y_1 = b_0 + b_1X_1 + b_2X_2 + b_3X_3 + b_{12}X_1X_2 + \ldots + b_nX_n$$

Where;
Y_1 - Response;
Y_2 - Intercept;
b_1 to b_n - Regression coefficients;
X_1, X_2, X_3 - Independent variable

Table 1 Variables and levels as per BBD

Variables	**Levels used**	
Independent variables	**Low (-)**	**High (+)**
X_1 - Stearyl alcohol (mg)	285	430
X_2 - Span 60 (mg)	100	280
X_3 - Tween 60 (mg)	250	300
Dependent variable/response		
Y_1- Particle size (μm)		
Y_2 - Percent encapsulation efficiency (%EE)		
Y_3 – Zeta potential (mV)		

Table 2 Possible trial CUR-SLNs formulations generated as per BBD

Trials	CUR (mg)	Factors with levels (mg)		
		Span 60	Tween 60	Stearyl alcohol
1	100	430	280	275
2	100	430	190	250
3	100	357.5	100	300
4	100	357.5	190	275
5	100	430	190	300
6	100	285	100	275
7	100	357.5	190	275
8	100	285	280	275
9	100	285	190	250
10	100	357.5	100	250
11	100	357.5	280	250
12	100	357.5	190	275
13	100	285	190	300
14	100	357.5	280	300
15	100	430	100	275

- **Preparation of CUR-SLNs:** CUR-SLNs were prepared by nano emulsion template method[25] with slight modification. Concisely, the mixture of CUR/Stearyl alcohol/Tween 60/Span 60/Brij 35 at different weight proportions as shown in the table 8 were melted in a water bath at 70°C. Filtered deionized water was preheated at 70 °C and was added (5 ml) to molten mixture with continuous magnetic stirring at 800 rpm for 30 min to obtain a clear nano emulsion. The temperature was maintained at 70°C during the production of nano emulsion. Subsequently, hot nano emulsion was rapidly cooled down at 4°C in crushed ice box with continuous stirring at 800 rpm to accomplish solidification of lipid to form CUR-SLNs, further they were kept at 4 °C for further analysis.

2.2. Evaluation

- **FTIR studies:** The FTIR spectra for CUR and optimal CUR-SLNs were recorded using BRUKER-FTIR spectrophotometer in the wave number region from 4000 cm^{-1} to 500 cm^{-1}.
- **Experimental design:** Box Behnken Design was used to conduct all the experiments and suggested formulations were developed and analyzed for selected responses. Study of variance (ANOVA) was used to conduct the statistical analysis of variables to see formulation variable and their interaction. Check the influence of variables affected the outcomes. Using sequential p-value, lack of fit p-value, adjusted R^2, and predicted R^2, the Design Expert® software determined the best-fitting model. P-values < 0.05 and F-values greater than 0.05 indicate that each component has a significant contribution[26]. The connection between causes and effects can be visualized using contour and 3-D surface graphs[27]. In a polynomial equation, a diminishing effect on the response is represented by a negative sign for the magnitude of the coefficient and an increasing effect by a positive sign[28].
- **Particle size and size distribution studies:** For all the batches of CUR-SLNs size analysis was carried out using Malvern Zetasizer Nano ZS (Malvern Instruments, UK). The freshly prepared CUR-SLNs were dispersed in double distilled water (DDW) and was used to characterize the vesicle size. Polydispersity Index (PDI) was also determined as a measure of homogeneity. Zeta potential of the CUR-SLNs was determined to estimate stability of the formulations.
- **Entrapment efficiency:** The percentage of entrapped CUR in SLNs was determined by exhaustive dialysis method. During the study the dialysis cellophane membrane was mounted between the donor and receptor compartment and the receptor medium was phosphate buffer pH 6.8, CUR-SLNs was placed on dialysis membrane. The whole assemble was kept on magnetic stirrer stirred the receptor medium. After 6 hr the

curcumin content in receptor compartment was determined by measuring absorbance at 429 nm using double beam UV spectrophotometer. The percent entrapment efficiency was calculated by using following equation.

$$\% \text{ Entrapment efficiency} = \frac{\text{Total drug} - \text{Free drug}}{\text{Total drug}}$$

- ***In vitro* drug release studies:** The drug release from CUR-SLNs were performed using Franz-diffusion cell. The dialysis cellophane membrane was mounted between the donor and receptor compartment and receptor medium was phosphate buffer pH 6.8, CUR-SLNs was placed on one side of the dialysis membrane. The whole assemble was kept on magnetic stirrer, at different intervals of time adequate samples were withdrawn, the drug release was determined by UV spectroscopic method. The *in vitro* drug release from the CUR-SLNs was computed by using dissolution software PCP Disso V3.
- **Fabrication of CUR-SLNs carbopol gel:** The optimized CUR-SLNs was incorporated into 1% w/w carbopol gel[29]. During loading, first plain carbopol gel was prepared by transferring accurately weighed amount of carbopol in measured amount of distilled water, the mixture was sonicate for 6-8 min to dissolve carbopol completely and avoid any airdrops. Further, the mixture is neutralized with triethanolamine to attain the desire pH. In later stage carefully incorporate optimized CUR loaded SLNs with constant stirring. The fabricated CUR-SLNs loaded were evaluated for their *in vitro* drug permeation, *ex vivo* permeation and skin irritant property.
- ***In vitro* drug permeation study:** *In vitro* permeation studies on Optimized CUR-SLNs loaded Carbopol gel was performed using Franz-diffusion cell. The dialysis cellophane membrane was mounted between the donor and receptor compartment. The receptor medium was phosphate saline buffer pH 6.8. A CUR-SLNs loaded Carbopol gel equivalent to 10 mg of CUR was placed on one side of the dialysis membrane. The receptor compartment was surrounded by a water jacket to maintain the temperature at 37 ±1°C. A Teflon coated magnetic bead operated to a magnetic stirrer stirred the receptor fluid. Periodically remove the samples and replaced immediately with an equal volume of receptor media for drug content determination by UV method at 428 nm. Compute the *in vitro* drug release from the CUR -SLNs by using dissolution software PCP Disso V3.
- ***Ex vivo* permeation study:** *Ex vivo* permeation was carried out using male Albino Wister rat skin as reported by Ibrahim et al[30] (figure 1). The permeation was conducted by using Franz diffusion cell, the rat skin was mounted between the donor and receptor compartment with the stratum corneum facing upper side on the diffusion cell. The diffusion area of the cell was 1.41 cm^2 and 20 ml phosphate buffer pH 6.8 taken in receptor compartment, temperature maintained at 37 ± 1°C. A CUR-SLNs loaded Carbopol gel equivalent to 10 mg of CUR was speeded over the rat skin. The receptor compartment content stirred in a magnetic stirrer. Periodically collect samples and were immediately replaced with the fresh media. Determine drug content from the samples by UV spectrophotometer at 428 nm. The cumulative amount of drug permeated (Q) at different time intervals were calculated using appropriate equations[31,32].

$$\text{Permeability coefficient } (K_p) = \frac{\text{Flux}}{\text{Initial concentration of drug in donor chamber}} = \frac{J_{ss}}{D_o}$$

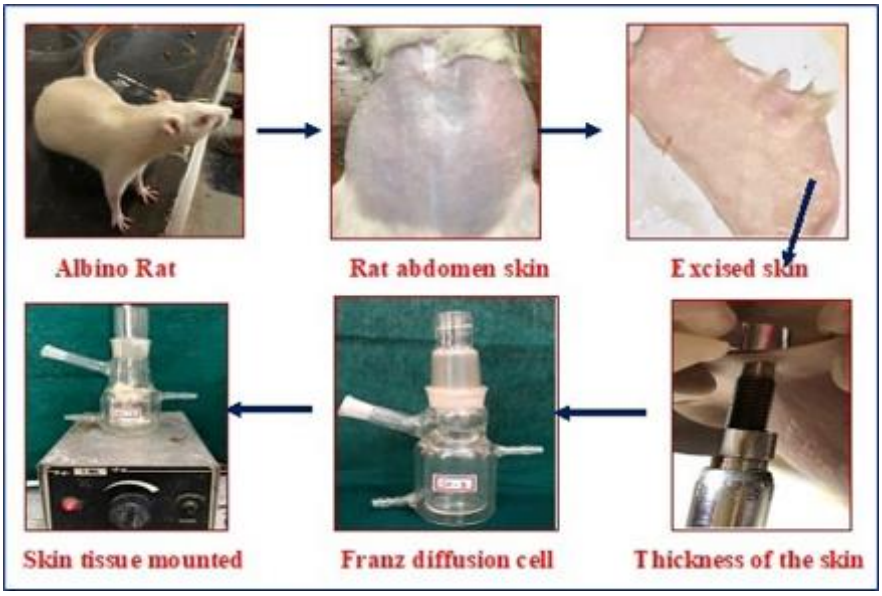

Figure 1 Schematic diagram of *ex vivo* permeation study

- **Skin irritation studies:** Skin irritation test was done as per Draize et al[33]. For the study Albino Wistar rats (200-250g) were selected and same was approved by University Animal Ethics Committee IAEC of V.L.College of Pharmacy, Karnataka, India (VLCP/IAEC/23-21,557/PO/Re/S/02/CCSEA)**.** All the animals used for the study were caged and maintained according to CPCSEA guidelines. The rats were divided into two groups (n = 4) as shown in figure 2. The rats were anesthetized and the abdominal area was shaved and wiped with 70 % alcohol swab. For Group - I apply CUR-Carbopol gel and Group – II apply optimized CUR-SLNs loaded carbopol gel. The skins were scored according to erythema and edema scale as 0 = none; 1 = slight; 2 = well defined; 3 = moderate; 4 = scar formation by visual observations.

Figure 2 Grouping of animals for skin irritation studies

3. Results and discussion

- **Preformulation studies:** The model drug CUR was subjected for preformulation studies such as solubility, melting point partition coefficient. The solubility of CUR complies with the standard values. The melting point was found to be 182^{o}C against standard 179-182^{0}C, partition coefficient (log P) was found to be 3.23 against the standard 3.44. The results were complies with the standard values indicate the drug sample was stable and pure.
- **FTIR studies:** FTIR spectra of CUR was shown in figure 3. FTIR spectra of CUR showed the characteristic peak at 2929.76 cm^{-1} (-OH stretching), 1739.88 cm^{-1} (C≡C stretching), 1623.88 cm^{-1} (CH=CH stretching, aromatic), 1593.75 cm^{-1}(CH_2 = CH_2 stretching, cyclohexyl) and 1270.15 cm^{-1} (C=O ester). The spectral data was ratified with literature indicate the CUR found to be pure and can be used for further studies. The characteristic FTIR peaks of CUR were found in optimized batch of CUR-SLNs indicates no interaction.

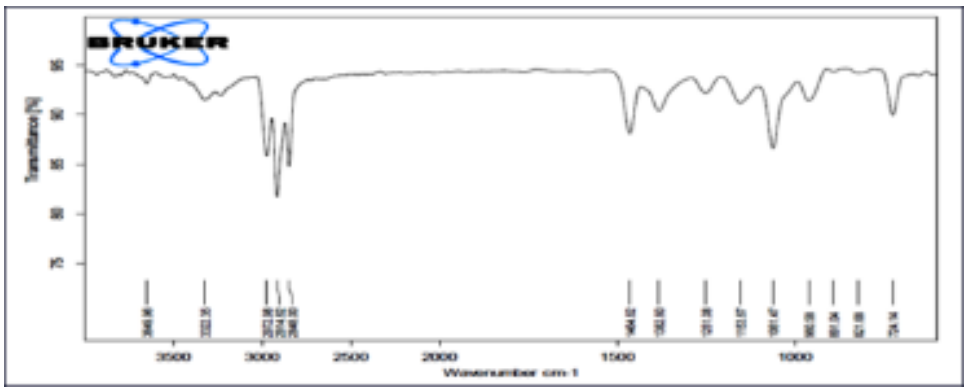

Figure 3 FTIR spectra of CUR

- **Analysis of BBD:** The relationships between independent variables viz., amount of Span 60 (X_1), amount of Tween 60 (X_2) and amount of Stearyl alcohol (X_3) at two levels (-1, +1), with dependent responses, such as % EE (Y_1), Particle size (Y_2) and Zeta potential (Y_3) were assessed by the BBD. The experiment response data was substituted in Design Expert Software and possible statistical data were generated as shown in table 3. The

relative models were found as the optimum models for all of the dependent responses. The significance of the model was estimated by ANOVA, where, at p-value < 0.05, the model is considered significant. The p-value < 0.05 clarifies that, the models generated were statistically significant to describe the interrelationship among the independent factors and the dependent responses.

Table 3 Experimental data of dependent response under the influence of independent variables as per BBD

Trial Runs	Response		
	Zeta potential (mV)	% EE	Particle size (nm)
1	-8.63	90.37	108.5
2	-7.67	86.2	123.23
3	-4.04	79.56	112.8
4	-3.21	77.12	185.3
5	-6.64	78.7	103.9
6	-9.43	84.49	234.3
7	-3.21	77.12	114.3
8	-7.67	83.33	236.47
9	-9.43	83.58	245.23
10	-3.2	88.8	154.32
11	-3.42	85.51	156.75
12	-3.21	77.12	114.32
13	-7.57	81.89	261.2
14	-1.49	79.15	123.45
15	-6.62	81.55	112.34

3.1. Effect of factors on Response Y_1 - Zeta potential

Table 4 ANOVA data for Response Y_1 - Zeta potential

Model	Sum of Squares	df	Mean Square	F-value	p-value
Significant	98.60	9	10.96	41.33	0.0004
A-Span 60	2.58	1	2.58	9.72	0.0263
B-Tween 60	0.5408	1	0.5408	2.04	0.2125
C-Stearyl alcohol	1.98	1	1.98	7.47	0.0411
AB	3.55	1	3.55	13.41	0.0146
AC	0.1722	1	0.1722	0.6498	0.4568
BC	1.92	1	1.92	7.24	0.0433
A^2	86.27	1	86.27	325.49	< 0.0001
B^2	0.0071	1	0.0071	0.0267	0.8767
C^2	0.1727	1	0.1727	0.6515	0.4563
Residual	1.33	5	0.2650		
Cor Total	99.93	14			

ANOVA suggested (Table 4) Quadratic model was suggested, here A, C, AB, BC, A^2 are significant model terms, nonsignificant lack of fit and low values of predicted residual sum of squares. The model F value of 41.33 implies the model is significant with p values less than 0.0500 there is only a 0.04% chance that an F-value this large could occur due to noise. The linearity plot of predicted value versus actual value of model condition Zeta potential was shown in figure 4. The linearity plot had good correlation i.e., R^2 - 0.9867. The Predicted R^2 of 0.7878 is in reasonable agreement with the Adjusted R^2 of 0.9629 indicates prediction results from the Design-Expert® program had precision and reliability. Adequate precision measures the signal to noise ratio. A ratio greater than 4 is desirable. The ratio of 19.6738 indicates an adequate signal, model used to navigate the design space. The relationship between factors vs response were shown in response surface plots viz., Contour and 3D surface and interaction between factors vs response was shown in figure 5. The polynomial equation was generated for actual factors. The equation in terms of actual factors can be used to make predictions about the response for given levels of each factor. Here, the levels should be specified in the original units for each factor.

Zeta potential = -108.57669 + 0.724283 Span 60 - 0.028059 Tween 60 - 0.187950 Stearyl alcohol - 0.000144 Span 60 * Tween 60 - 0.000114 Span 60 * Stearyl alcohol + 0.000308 Span 60^2 - 5.40123E-06 Tween 60^2 + 0.000346 Stearyl $alcohol^2$

Zeta potential is a measure of the effective electric charge on the nanoparticle's surface and quantifying electrostatic stabilization of nanoparticles. Therefore, it is an indirect measure of the physical stability of lipid nanoparticles. The magnitude of the zeta potential provides information about particle stability. The zeta potential values ranges from -9.43 mV (6^{th} and 9^{th} trial) -3.2 mV (10^{th} trial) indicating the negative surface charge and therefore no aggregation of particles was observed. The results suggest Span 60 has direct relation on zeta potential, as the concentration increases the zeta potential increases negatively further increase in concentration reduce the zeta potential negatively as shown in contour and 3D surface plots. All other factors has interaction effect along with Span 60 as indicated in interaction plots. A positive coefficient implies that the factor has a synergistic influence, whereas a negative value shows an antagonistic influence on the responses.

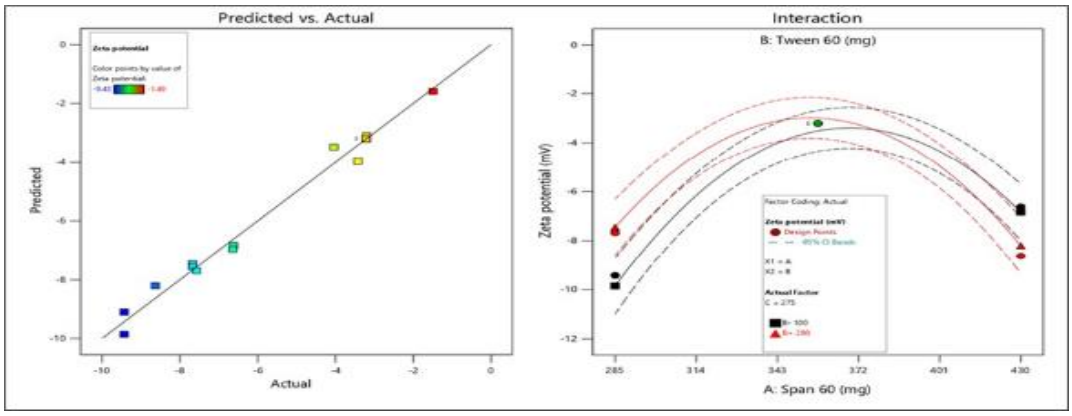

Figure 4 Diagnostic plots a) Predicted vs Actual b) Interaction

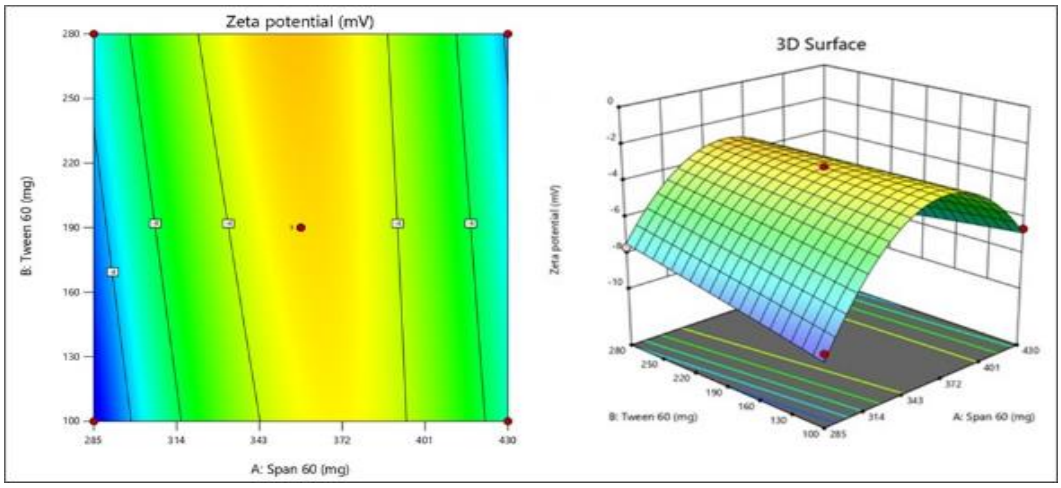

Figure 5 Response surface plots a) Contour b) 3D surface

3.2. Effect of factors on Response Y_2 - % EE

ANOVA suggested (Table 5) Quadratic model was suggested, here C, A^2, B^2 are significant model terms, nonsignificant lack of fit and low values of predicted residual sum of squares. The model F value of 5.28 implies the model is significant with p values less than 0.0500 there is only a 4.08 % chance that an F-value this large could occur due to noise. The linearity plot of predicted value versus actual value of model condition Zeta potential was shown in figure 6. The linearity plot had good correlation i.e., R^2 - 0.9048. The Predicted R^2 of 0.5434 is in reasonable agreement with the Adjusted R^2 of 0.7334 indicates prediction results from the Design-Expert® program had precision and reliability. Adequate precision measures the signal to noise ratio. A ratio greater than 4 is desirable. The ratio of 6.2877 indicates an adequate signal, model used to navigate the design space. The relationship between factors vs response were also shown in response surface plots viz., Contour and 3D surface (figure 7) and interaction between factors vs response was shown in figure 6. The polynomial equation was generated for actual factors. The equation in terms of actual factors can be used to make predictions about the response for given levels of each factor. Here, the levels should be specified in the original units for each factor.

Encapsulation efficiency = + 407.18703 - 0.332658 Span 60 - 0.418054 Tween 60 -1.56696 Stearyl alcohol + 0.000382 Span 60 * Tween 60 - 0.000801 Span 60 * Stearyl alcohol + 0.000320 Tween 60 * Stearyl alcohol + 0.000680 Span 60^2 + 0.000523 Tween 60^2 + 0.003034 Stearyl $alcohol^2$.

The encapsulation efficiency is the measure of drug loading in the nanoparticles, the magnitude of % EE provides information about drug loading and drug content within the nanoparticles. The % EE ranges from 77.12 (4, 7 and 11 trial) to 90.37 (trial 1). The concentration of Stearyl alcohol and combination of Span 60 and tween 60 has significant influence on % EE. As the concentration of Span 60 and Tween 60 increases the % EE was increases linearly and shows synergistic effect between the factors on stated response as shown in interaction plot. A positive coefficient implies that the factor has a synergistic influence, whereas a negative value shows an antagonistic influence on the responses.

Table 5 ANOVA data for Response Y_2 - % EE

Model	Sum of Squares	df	Mean Square	F-value	p-value
Significant	228.01	9	25.33	5.28	0.0408
A-Span 60	1.56	1	1.56	0.3246	0.5935
B-Tween 60	1.96	1	1.96	0.4085	0.5509
C-Stearyl alcohol	76.82	1	76.82	16.01	0.0103
AB	24.90	1	24.90	5.19	0.0717
AC	8.44	1	8.44	1.76	0.2421
BC	2.07	1	2.07	0.4321	0.5400
A^2	47.22	1	47.22	9.84	0.0258
B^2	66.34	1	66.34	13.82	0.0137
C^2	13.28	1	13.28	2.77	0.1571

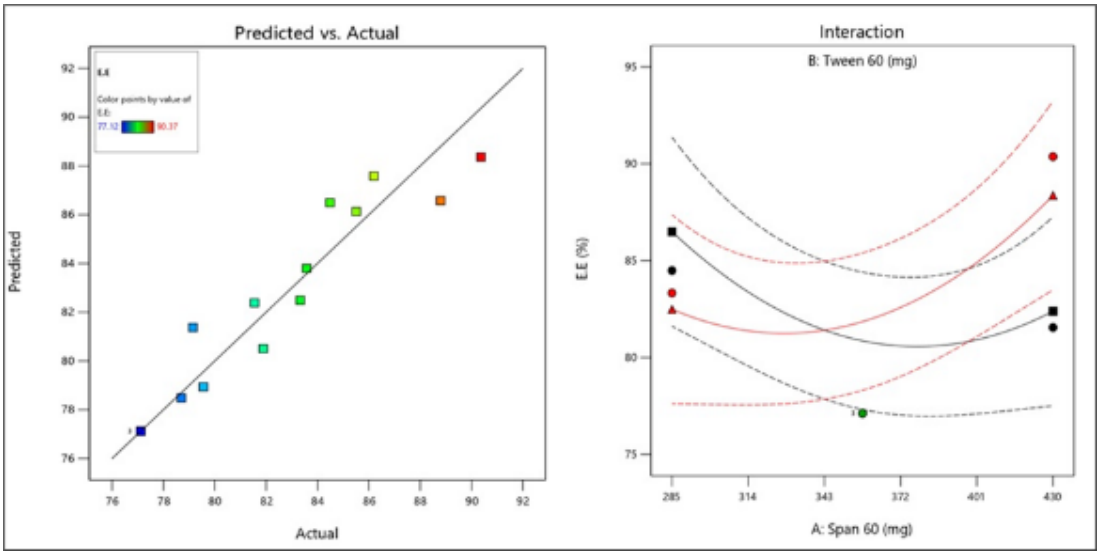

Figure 6 Diagnostic plots a) Predicted vs Actual b) Interaction

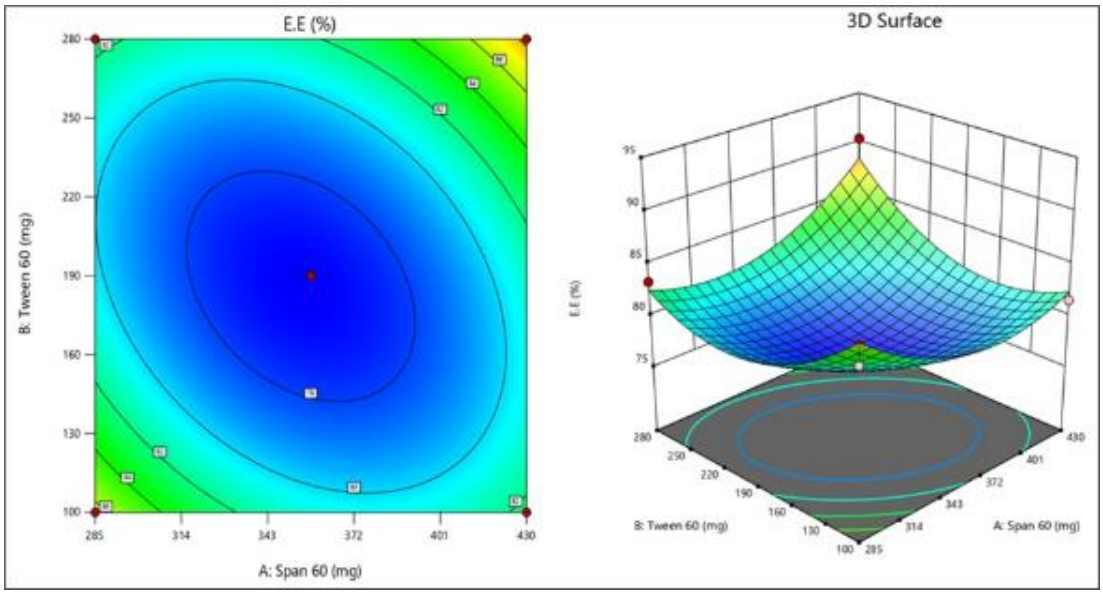

Figure 7 Response surface plots a) Contour b) 3D surface

3.3. Effect of factors on Response Y3 – Particle size

ANOVA suggested (Table 6) linear model was suggested, here A is significant model term, nonsignificant lack of fit and low values of predicted residual sum of squares. The model F value of 12.02 implies the model is significant with p values less than 0.0500 there is only a 0.09 % chance that an F-value this large could occur due to noise.

Table 6 ANOVA data for Response Y_3 – Particle size

Model	Sum of Squares	df	Mean Square	F-value	p-value
Significant	35790.84	3	11930.28	12.02	0.0009
A-Span 60	35010.55	1	35010.55	35.28	< 0.0001
B-Tween 60	16.27	1	16.27	0.0164	0.9004

C-Stearyl alcohol	764.01	1	764.01	0.7699	0.3990
Residual	10915.37	11	992.31		
Pure Error	3359.72	2	1679.86		
Cor Total	46706.21	14			

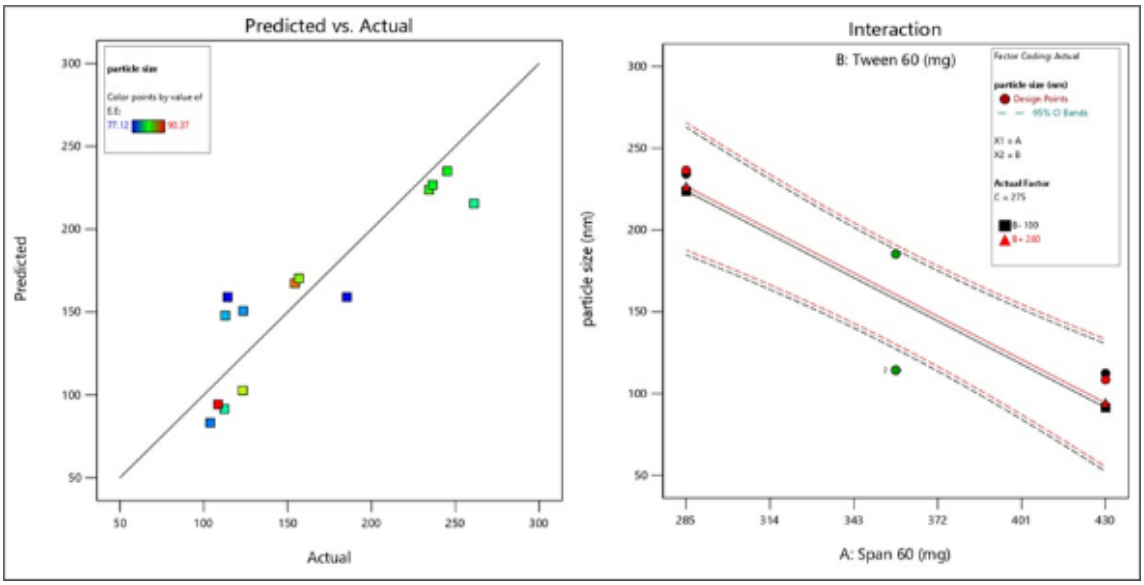

Figure 8 Diagnostic plots a) Predicted vs Actual b) Interaction

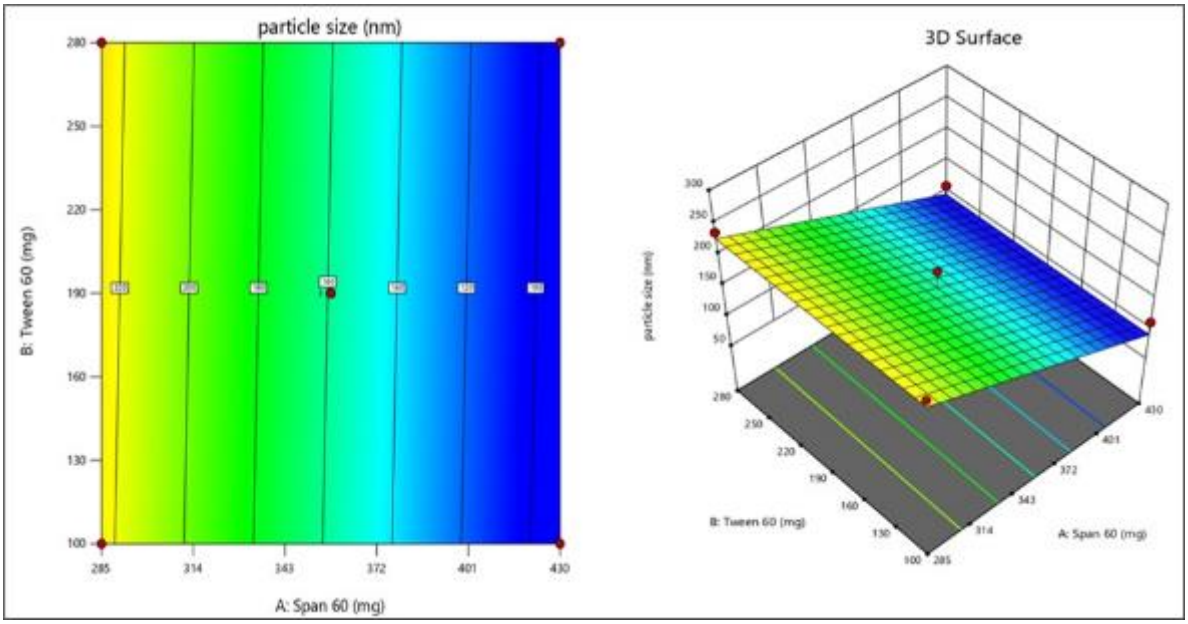

Figure 9 Response surface plots a) Contour b) 3D surface

The linearity plot of predicted value versus actual value of model condition Zeta potential was shown in figure 8. The linearity plot had good correlation i.e., R^2 - 0.7663. The Predicted R^2 of 0.5995 is in reasonable agreement with the Adjusted R^2 of 0.7026 indicates prediction results from the Design-Expert® program had precision and reliability. Adequate precision measures the signal to noise ratio. A ratio greater than 4 is desirable. The ratio of 9.335 indicates an adequate signal, model used to navigate the design space. The relationship between factors vs response were shown in response surface plots viz., Contour and 3D surface (figure 9) and interaction between factors vs response was shown in figure 8. The polynomial equation was generated for actual factors. The equation in terms of actual factors can be

used to make predictions about the response for given levels of each factor. Here, the levels should be specified in the original units for each factor.

Particle size = + 589.78695 - 0.912466 Span 60 + 0.015847 Tween 60 - 0.390900 Stearyl alcohol

The particle size of nanoparticle is ranging from 103.9 (trial 5) to 261.2 (trial 13) and was directly influenced by the concentration of Span 60. As the concentrations of Span 60 increases the particle size increases at lower concentrations produce smaller size nanoparticles. A positive coefficient implies that the factor has a synergistic influence, whereas a negative value shows an antagonistic influence on the responses and no interaction among factors. In Nano delivery the size of the particle is the measure of permeation across the biological barriers in systemic delivery as well as transdermal delivery. Nanoparticles with diameter less than 300 nm are able to deliver their contents to some extent into the deeper skin layers. Particles in the size range of 100 to 210 nm, may preferentially penetrate through the transfollicular route.

3.4. Numerical optimization

A numerical optimization technique using the desirability approach was employed to develop an optimized formulation with the desired responses. Fix the constraints for factors viz., maximize the X_1 (Span 60) and X_2 (Tween 60), in range for X_3 (Stearyl alcohol); for response, set in range Y1 (zeta potential), maximizing Y2 (% EE) and minimizing Y3 (Particle size). Optimize the constraints by using Deign Expert software to generate the possible solution with high degree of desirability and generate the possible overlay plot to explain the details of the optimized batch. The point prediction method confirms the ratio of X_1, X_2 and X_3 and confirmed by predicted response at 95% CI as shown in table. The Over lay plot in figure 10 and desirability of constraints factors shown in figure 11, provides optimized batch with predicted response. The optimum formulation generated as per BBD, comprising of X_1-Span 60 (430 mg), X_2-Tween 60 (280 mg) and X_3-Stearyl alcohol (262.069 mg), with predicted response of -8.65009 (Y_1- Zeta potential), 90.8499 (Y_2- % EE) and 99.43 nm (Y_3-Particle size). The optimized formula was validated by formulating and evaluating CUR-SLNs, the relative data was given the tables 7 and figure 12, 13. The experimental results validate and ratified with predicted data, it clearly indicates the DoE studies can be used to study the influence of three factor on three responses. Validation of the predicted values of responses was performed by comparing with the experimental data, which indicated high degree closeness between the predicted and experimental values and confirmed excellent prognostic ability of the employed mathematical model.

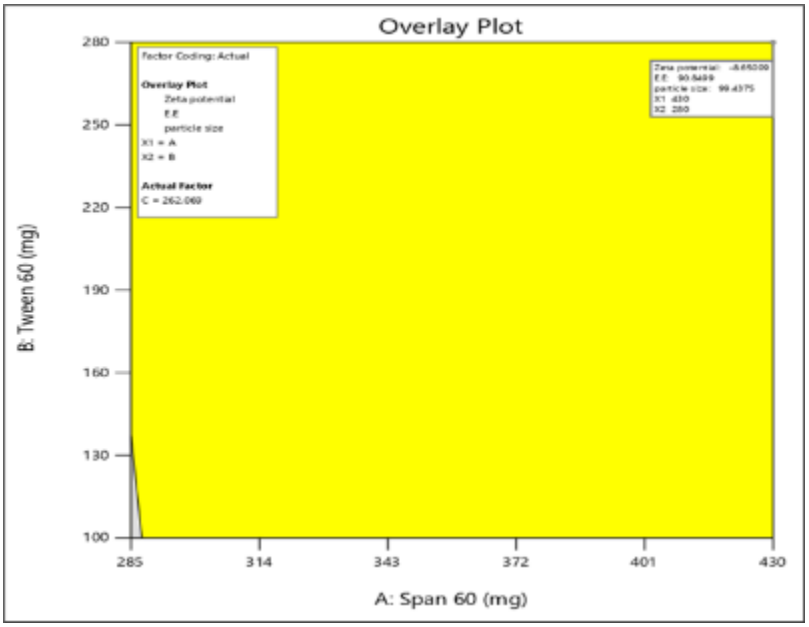

Figure 10 Over lay plot of desirability factors and predicted response

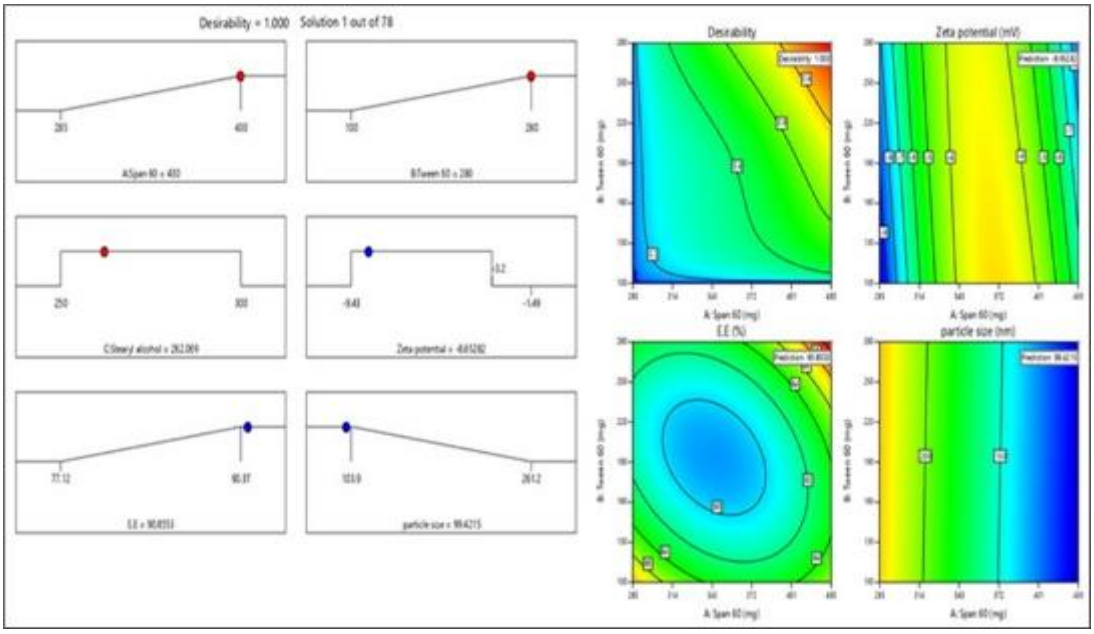

Figure 11 Desirability plots of all factors on all response

Table 7 Formulae of OP-CUR-SLNs as pre BBD and its comparative evaluation data

OP-CUR-SLNs		**Comparative data**		
Ingredients (mg)	**OP-CUR-SLNs**	**Parameter**	**Predicted**	**Experimental**
CUR	100	% EE	90.84	88.23±1.102
Span 60	430	Particle size (nm)	195.43	214.3
Stearyl alcohol	262.069	Zeta potential (mV)	-8.65009	-9.43
Tween	280	t_{50} (hr)	-----	25.22 hr
Brij 35	860	Q_{48} (hr)	-----	98.65±0.22%

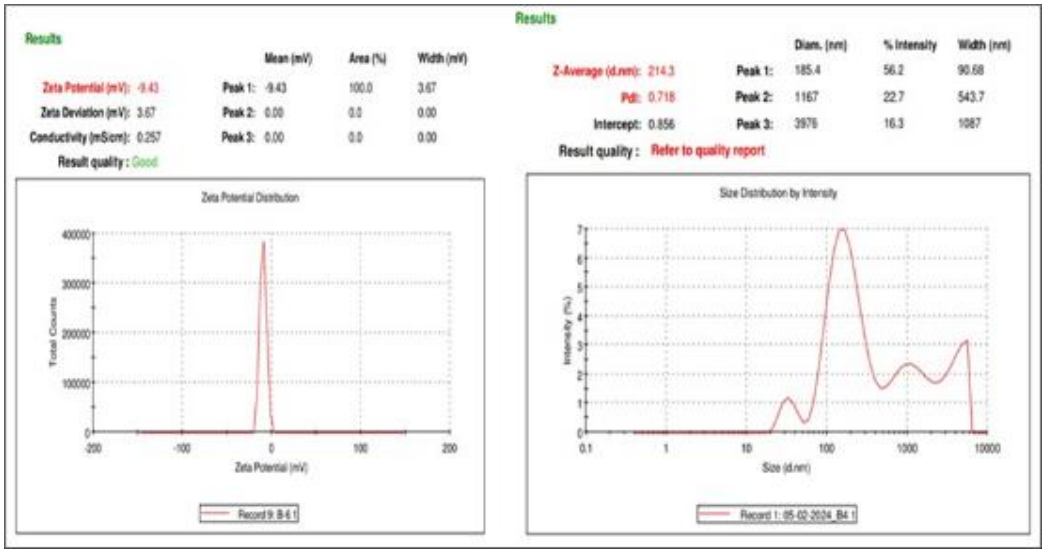

Figure 12 Experimental zeta potential and particle size of OP-CUR-SLNs

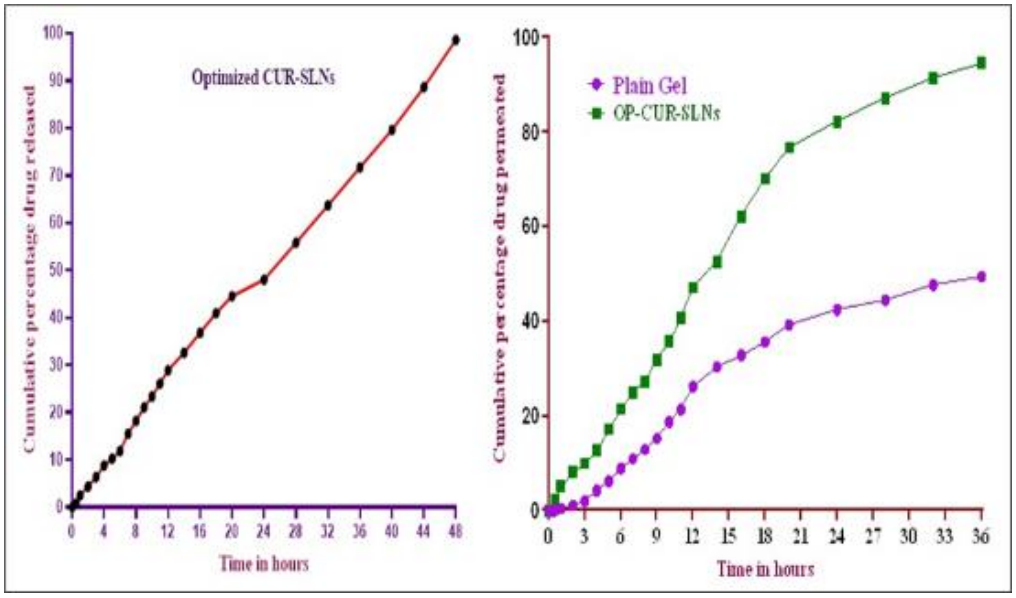

Figure 13 Drug release profile a) in vitro drug release b) Ex vivo drug permeated across rat skin

3.5. *In vitro* drug release

The cumulative percent drug release of OP-CUR-SLNs was found to be, 11.845 ± 0.22 after 6 hr, faster drug release at 6 hr may be due to release of drugs from the adhered particles. After 12 hr the drug release was steady and found to be 28.908 ± 0.07 due complete exhaust of adhered drug particles from the OP-CUR-SLNs. The drug release was steady and controlled for 48 hr and was found to be, 98.52 ± 0.58 (figure 13). The *in vitro* drug release data for OP-CUR-SLNs was further fitted into various kinetic equations to find out the order and mechanism of drug release and the model fitted data, the correlation coefficient showed that the release profile followed the first order, also from Korsmeyer peppas model, the release exponent, n was found to be greater than 0.5 indicated the drug release followed non fickian and release mechanism was indicative of erosion followed by diffusion controlled.

3.6. *Ex vivo* permeation study

The OP-CUR-SLNs was further studied for their ability to permeate across the skin barriers by fabricate into carbopol gel. The OP-CUR-SLNs equivalent to 10 mg of CUR was incorporated into 1% carbopol gels and evaluated for *ex vivo* permeation and skin irritation test. Further the data was compared with CUR loaded plain carbopol gel to assess the efficiency of permeation of SLNs over plain. *Ex vivo* permeation studies predicted the *in vivo* permeation behaviour of the formulations when it was subjected to the transdermal applications. The amount of the drug permeated gives the information about the amount of drug absorbed into the blood. The skin permeation of CUR from the optimized formulation CUR-SLNs and plain gel was performed using skins obtained from the Wistar Albino rats using Franz diffusion cell (figure 13). After 36 h of the study period, only 49.50 ± 0.28 % of CUR was permeated from the plain gel thorough the rat skin, whereas the carbopol gel loaded with OP-CUR-SLNs shows 94.62 ± 0.20 % CUR permeation across the rat skin. The results clearly indicate that SLNs possess higher skin penetration ability. The comparative low skin permeability of CUR in plain gel was due to its lower aqueous solubility, while the high permeability of SLNs resulted in improved skin penetration of CUR. The *ex-vivo* study performed using rat skin revealed that cumulative drug release from OP-CUR-SLNs showed maximum flux i.e. 60.68 ± 18 µg/cm^2/h. Better transdermal flux without lag phase of SLNs might be the result of one or more of the wing mechanisms as reported previously i.e. increased solubility of active drug, high association of drugs with lipid layers of nanoparticles. Apart from the amount of surfactant viz., Span 60 and Tween 60 in SLNs modifies the structural composition of stratum corneum and increases the thermodynamic activity of the drug as well as skin vesicular partitioning. Moreover, the presence of unsaturated double bond in the oleate side chain of Span 60 was responsible for the significant enhancement of CUR permeation. The packing nature of unsaturated fatty acids changes the stratum corneum lipid structure upon binding to the keratin filament, hence increase drug permeability across skin.

3.7. Skin irritation Test

The Albino rats received optimal gels as well as plain gel were free from of any irritation and there were no signs of erythema (table 8). According to Draize et al, the optimal proniosomal gels and plain gels considered to be non-irritant and the optimal proniosomal gel formula is safe to be applied on the skin for the intended period of time. The Span 60

and Stearyl alcohol used in the preparation of SLNs were mild, a finding consistent with the drug design principle of Quality by Design (QbD).

Table 8 The irritation scores of OP-CUR-SLNs and CUR plain gel on normal rat skin

Formulation	Application period/ Erythema scores						
	Day-1	Day-2	Day-3	Day-4	Day-5	Day-6	Day-7
OP-CUR-SLNs	0	0	0	0	0	0	0
CUR-Plain gel	0	0	0	0	0	0	0

3.8. Stability Study

The short-term stability of OP-CUR-SLNs was carried out for three months as per ICH guidelines. There was no evident for aggregation, during the study period and it was found that the OP-CUR-SLNs were able to retain their structure. At refrigerated condition (4±2 °C) OP-CUR-SLNs shown 97.14 ± 1.132% drug content; 84.32 ± 0.69% encapsulation efficiency; at room temperature (25±2 °C) shown 97.11 ± 0.79 % drug content and 86.88 ± 0.99 % encapsulation efficiency and thus it was found that storage under refrigerated condition showed greater stability. In both the storage conditions percent drug content, percent encapsulation efficiency was within the specification throughout the study period.

4. Conclusion

Response surface BBD can be successfully applied to formulate and optimize Curcumin loaded SLNs and were conveniently prepared by nano-emulsion template method. The statistical tests in design experiment conclude that some linear and interaction terms of independent variables influence on the response. The numerical optimization was successfully used to generate optimized formula can be validated within the design space. The OP-CUR-SLNs exhibited good entrapment efficiency and particle size. Further the OP-CUR-SLNs loaded transdermal carbopol gel shows good *in vitro* drug release and better *ex vivo* permeation than the plain CUR loaded gel, which concludes CUR-SLNs considered to be a successful topical transdermal drug delivery system and provide a sustained release of encapsulated drug. Furthermore, CUR-SLNs loaded carbopol gel considered to be non-irritant and safe to be applied on the skin for the intended period of time.

Compliance with ethical standards

Acknowledgments

We wish to thanks to the principal and management of V. L. College of pharmacy for providing the facilities to carry out the work.

Disclosure of conflict of interest

There are no conflicts of interest.

Statement of ethical approval

The University Animal Ethics Committee IAEC of V.L. College of Pharmacy, Karnataka, India (VLCP/IAEC/23-21,557/PO/Re/S/02/CCSEA), approved the study protocol.

References

[1] Lee WH, Loo CY, Bebawy M, Luk F, Mason R, Rohanizadeh R. Curcumin and its derivatives: their application in neuropharmacology and neuroscience in the 21st century. Cur Neuropharmacol 2013; 11: 338-378.

[2] Mahmud M, Piwoni A, Filiczak N, Janicka M, Gubernator J. Long circulating curcumin loaded liposome formulations with high incorporation efficiency, stability and anticancer activity towards pancreatic adenocarcinoma cell lines in vitro. PLoS One 2016; 11:e0167787.

[3] Shahani K, Swaminathan SK, Freeman D, Blum A, Ma L, Panyam J. Injectable sustained release microparticles of curcumin: a new concept for cancer chemoprevention. Cancer Res 2010; 70: 4443-4452.

[4] Jankun J, Wyganowska-Swiątkowska M, Dettlaff K, Jelinska A, Surdacka A, Wątrobska Swietlikowska D et al. Determining whether curcumin degradation /consideration is actually bioactivation (Review). Int J Mol Med 2016; 37:1151- 1158.

[5] Pescosolido N, Giannotti R, Plateroti AM, Pascarella A, Nebbioso M. Curcumin: therapeutical potential in ophthalmology. Planta Med 2014; 80:249-254.

[6] Chetoni P, Burgalassi S, Monti D, Tampucci S, Tullio V, Cuffini AM et al. Solid lipid nanoparticles as promising tool for intraocular tobramycin delivery: Pharmacokinetic studies on rabbits. Eur J Pharm Biopharm 2016; 109: 214-223.

[7] Yadav M, Schiavone N, Guzman AA, Giansanti F, Papucci L, Perez de Lara MJ. Atorvastatin-loaded solid lipid nanoparticles as eye drops: Proposed treatment option for age-related macular degeneration (AMD). Drug Deli Tran Res 2020; 10: 919-944.

[8] Huang S, He J, Cao L, Lin H, Zhang W, Zhong Q. Improved physicochemical properties of curcumin-loaded solid lipid nanoparticles stabilized by sodium caseinate-lactose Maillard conjugate. J Agric Food Chem 2020; 68: 7072-7081.

[9] Kumar PS, Punniamurthy N. Formulation development and characterization of curcumin loaded solid lipid nanoparticles for improved aqueous solubility and bioavailability. J Pharm Innovation 2017; 6(4):7-11.

[10] Teixeira ACT, Fernandes AC, Garcia AR, Ilharco LM, Brogueira P, Da Silva AMP. Microdomains in mixed monolayers of oleanolic and stearic acids: thermodynamic study and BAM observation at the air-water interface and AFM and FTIR analysis of LB monolayers. Chem Phys Lipids 2007; 149: 1-13.

[11] Muangnoi C, Jithavech P, Ratnatilaka Na Bhuket P, Supasena W, Wichitnithad W, Towiwat P. A curcumin-diglutaric acid conjugated prodrug with improved water solubility and antinociceptive properties compared to curcumin. Biosci Biotechn Biochem 2018; 82: 1301-1308.

[12] Li L, Braiteh FS, Kurzrock R. Liposome-encapsulated curcumin: in vitro and in vivo effects on proliferation, apoptosis, signaling, and angiogenesis. Cancer 2005;104: 1322-1331.

[13] Salmazi R, Calixto G, Bernegossi J, Dos Santos Ramos MA, Bauab TM, Chorilli M. A curcumin-loaded liquid crystal precursor mucoadhesive system for the treatment of vaginal candidiasis. Int J Nanomed 2015; 10:4815-4824.

[14] Sari TP, Mann B, Kumar R, Singh RRB, Sharma R, Bhardwaj M et al. Preparation and characterization of nanoemulsion encapsulating curcumin. Food Hydrocolloids 2015; 43:540-546.

[15] Liu A, Lou H, Zhao L, Fan P. Validated LC/MS/MS assay for curcumin and tetrahydrocurcumin in rat plasma and application to pharmacokinetic study of phospholipid complex of curcumin. J Pharm Biomed Anal 2006; 40: 720-727.

[16] Nahar PP, Slitt AL, Seeram NP. Anti-inflammatory effects of novel standardized solid lipid curcumin formulations. J Med Food 2015;18:786-792.

[17] Araya-Sibaja AM, Salazar-Lopez NJ, Romero KW, Vega-Baudrit JR, Domínguez-Avila JA, Contreras CA. Use of nanosystems to improve the anticancer effects of curcumin. Beilstein J Nanotechnol 2021; 12: 1047-1062.

[18] Pashkovskaya AA, Vazdar M, Zimmermann L, Jovanovic O, Pohl P, Pohl EE. Mechanism of long-chain free fatty acid protonation at the membrane-water interface. Biophys J 2018; 114: 2142-2151.

[19] Muller RH, Mader K, Gohla S. Solid lipid nanoparticles (SLN) for controlled drug delivery–a review of the state of the art. Eur J Pharm Biopharm 2000; 50: 161-177.

[20] Rostamkalaei SS, Akbari J, Saeedi M, Morteza-Semnani K, Nokhodchi A. Topical gel of Metformin solid lipid nanoparticles: a hopeful promise as a dermal delivery system. Colloids Surf B Biointerfaces 2019; 175: 150-157.

[21] Ahmed TA, Badr-Eldin SM, Ahmed OAA, Aldawsari H. Intranasal optimized solid lipid nanoparticles loaded in situ gel for enhancing trans-mucosal. J Drug Deli Sci Tech 2018; 48: 499-508.

[22] Mahanat S, Kumar S, Nanda S, Rao R. Microsponges for dermatological applications: Perspectives and challenges. Asian J Pharm Sci 2020; 15 (3): 273-291.

[23] Yang Q, Zhong W, Xu L, Li H, Yan Q, She Y et al. Recent progress of 3D-printed microneedles for transdermal drug delivery. Int J Pharm 2021; 593:120106.

[24] Chavda VP. Applications of targeted nano drugs and delivery systems. Nanosci Nanotechnol Drug Deli 2019; 18: 69-92.

[25] Koroleva M, Portnaya I, Mischenko E, Abutbul-Ionita I, Kolik-Shmuel L, Danino D. Solid lipid nanoparticles and nanoemulsions with solid shell: Physical and thermal stability. J. Colloid Interface Sci. 2022, 610, 61–69.

[26] Behbahani ES, Ghaedi M, Abbaspour M, Rostamizadeh MK. Optimization and characterization of ultrasound assisted preparation of curcumin-loaded solid lipid nanoparticles: Application of central composite design, thermal analysis and X-ray diffraction techniques Ultrason. Sonochem 2017; 38: 271-280.

[27] Dudhipala N, Janga KY. Lipid nanoparticles of Zaleplon for improved oral delivery by Box-Behnken design: optimization, in vitro and in vivo evaluation Drug Dev Ind Pharm 2017; 43:1205-1214.

[28] Alhalmi A, Amin S, Beg S, Al-Salahi R, Mir SR, Kohli K. Formulation and optimization of naringin loaded nanostructured lipid carriers using Box-Behnken based design: In vitro and ex vivo evaluation. J Drug Deli Sci Tech 2022; 74:103590.

[29] Takahashi Yet al. Trial for transdermal administration of sulfonyl ureas. J Pharm Soc Japan 1997; 117: 1022-1027.

[30] Eorthy PH, Patel MS. Demonstration of maximum solubilization in a polyoxy ethylene alkylether series of non-ionic surfactants. J Pharm Pharmacol 1982;34: 543-546.

[31] Abdel Rahman AA et al. Factors affecting chlordiazepoxide solubilization by non-ionic surfactants. Bull Pharm Sci Assiut Univ 1991;14(1-2): 35-45.

[32] Mueller-Goymann CC, Usselmann BS. Solubilization of cholesterol in liquid crystals of aqueous systems of poly oxyethylene cetyl ethers. Acta Pharm Jugosl 1988; 38(4): 327-329.